Impact of the modulation doping layer on the ν=5/2 anisotropy

X. Shi, W. Pan, K. W. Baldwin, K. W. West, L. N. Pfeiffer, and D. C. Tsui

Phys. Rev. B **91**, 125308 — Published 30 March 2015

DOI: 10.1103/PhysRevB.91.125308

Impact of Modulation Doping Layer on the ν=5/2 Anisotropy

X. Shi[1], W. Pan[1], K.W. Baldwin[2], K.W. West[2], L.N. Pfeiffer[2], and D.C. Tsui[2]

[1] Sandia National Labs, Albuquerque, New Mexico 87185, USA
[2] Princeton University, Princeton, New Jersey 08544, USA

Abstract:

We have carried out a systematic study of the tilted magnetic field induced anisotropy at Landau level filling ν=5/2 in a series of high quality GaAs quantum wells, where the setback distance (d) between the modulation doping layer and the GaAs quantum well is varied from 33 to 164 nm. We have observed that in the sample of the smallest d electronic transport is anisotropic when the in-plane magnetic field (B_{ip}) is parallel to [1-10] crystallographic direction, but remains more or less isotropic when B_{ip} // [110]. In contrast, in the sample of largest d, electronic transport is anisotropic in both crystallographic directions. Our results clearly show that the modulation doping layer plays an important role in the tilted field induced ν=5/2 anisotropy.

The modulation doping scheme was invented nearly 40 years ago [1] to achieve high electron mobility in GaAs quantum wells. This invention has had enormous impact on our daily life and scientific discoveries. Indeed, it is hard to imagine any cell phone without high electron mobility transistors, which are the direct outcome of the modulation doping invention.

Scientifically, the introduction and perfection of modulation doping made it possible to increase the electron mobility of the two-dimensional electron system (2DES) from merely ~ 10,000 cm^2/Vs in the late 70's to ~ 40,000,000 cm^2/Vs a few years ago [2]. One of many surprising discoveries enabled by this increase in electron mobility is the fractional quantum Hall effect (FQHE) [3], where the 2D electrons form a new incompressible liquid caused by strong electron-electron interactions. Since the first observation of the FQHE at the Landau level filling factor $\nu=1/3$, a total of 80 some FQHE states have been identified and almost all of them can be understood within the Laughlin wavefunction [4], hierarchy [5,6] and composite fermion (CF) [7] models.

For a long time, the role of modulation doping on the FQHE was to increase electron mobility and, thus, to magnify the electron-electron interaction effect and to uncover more fragile FQHE states. Recently, however, new roles played by modulation doping on may-body electron phases have been noted. For example, it was proposed that the possible quasiperiodic potential in the modulation doping layer might be the cause of the high-frequency magneto-oscillations around $\nu=1/2$ [8]. Moreover, it was observed that the long-range charged disorder potential fluctuations originated from modulation doping

layers were more detrimental to the stability of the ν=5/2 FQHE state than the short-range neutral disorder potential fluctuations [9, 10, 11].

In this Letter, we show convincing evidence that modulation doping layers play an important role in the anomalous behavior of the in-plane magnetic field (B_{ip}) induced anisotropy at the even-denominator 5/2 FQHE state. We report results from a systematic tilted magnetic field study in a series of high quality GaAs quantum wells, in which the impact of modulation doping layers on the 5/2 anisotropic phase is varied by changing the setback distance (d) between the modulation doping layers and the GaAs quantum well. We have observed that in the sample of the shortest d (or strongest impact of modulation doping) electronic transport is anisotropic when B_{ip} is parallel to [1-10] crystallographic direction, but remains more or less isotropic in the other direction of [110], consistent with previous work [12]. In contrast, in the sample of the largest d (or weakest impact of modulation doping), electronic transport is anisotropic in both crystallographic directions. Our results clearly show that the modulation doping layers do matter in the tilted magnetic field induced anisotropy in the 5/2 FQHE.

Among all the FQHE states, the 5/2 state remains the most exotic. In 1987, a strong minimum in the magneto-resistance R_{xx} and a plateau-like feature in the Hall resistance R_{xy} were observed at the even denominator filling factor ν=5/2 [13]. This state was confirmed unequivocally to be a true FQHE state 12 years later [14]. The observation of this even-denominator FQHE came as a total surprise, as it escapes the so-called odd-

denominator rule set by the Laughlin [4], hierarchy [5,6], and composite fermion [7] models. Now, it is generally believed that this state is due to the pairing of CFs [15].

The 5/2 state has been the center of FQHE research for more than 15 years. This state may be a Pfaffian state and, thus, its quasiparticles obey the non-abelian statistics. As a consequence, the 5/2 state can be used for topological quantum computation (QC) [16], which can have an enormous advantage over other QC approaches where error rate is relatively large. Extensive experimental work has been carried out to examine the spin polarization of the 5/2 state. The idea is quite straightforward. The 5/2 FQHE ground state must be fully spin polarized if the 5/2 state is a Pfaffian state. One of the most commonly used techniques to examine the spin polarization of a FQHE state is to tilt the sample in the magnetic field [17-22]. If spin polarized, the FQHE state would suffer almost no detrimental effect under tilt. However, if it is spin unpolarized or partially polarized, it can undergo a spin transition. The spin unpolarized FQHE is first destroyed and then reemerges as a spin polarized one. The first tilted magnetic field experiment [17] on the 5/2 state showed that the 5/2 state was quickly weakened and disappeared as the sample was tilted away from the sample normal. This result apparently favored a spin unpolarized ground stat at $\nu=5/2$. Later, in two experiments [18,19], it was observed that the disappearance of the 5/2 state was due to the transition from the FQHE state to an anisotropic state, probably a stripe state or a unidirectional charge density wave state. Finite size numerical calculations [23] further showed that the 5/2 FQHE and the anisotropic phases are very close in energy. An added in-plane magnetic field (B_{ip}) would make the 2DES effectively thinner and, hence, increase the ratio of V_1/V_3, where V_1 and

V_3 are Haldane pseudopotentials [23]. As a result, the anisotropic state becomes stable. Moreover, in these two experiments it was also demonstrated that the orientation of the 5/2 stripes was locked and always perpendicular to the direction of in-plane magnetic field [18,19,24-26], independent of crystallographic directions. However, in a recent report [12] in an extremely high density sample, this rotational symmetry was broken. Whether the tilted magnetic field induced anisotropy exists or not depended on GaAs crystallographic directions. Electronic transport became anisotropic when B_{ip} was parallel to [1-10] but remained isotropic if B_{ip} parallel to [110]. This observation is in contrast with the first two experiments, and its physics origin needs further exploration.

To this purpose, we have grown a series of GaAs modulation doped quantum wells with a fixed doping density but different set-back distance. The well width is kept at 20 nm, in order that only the lowest subband is occupied. The schematic of their growth structures is shown in Figure 1(a). This layer structure is the same for all the samples except for the set-back distance, d, which is varied from 33 to 164 nm. In Figure 1(b) we show the electron density and mobility as a function of the setback distance. It can be seen hat the electron density increases monotonically with decreasing d, while the mobility shows a non-monotonic d dependence, reaching a maximal value around d = 52 nm. In Figure 1(c), we show R_{xx} and R_{yy} in the d=52nm sample at zero tilt. Strong anisotropy is observed at half fillings ν=9/2 and 11/2 in the higher Landau levels. The hard (high resistance) axis is along [1-10] and easy (low resistance) axis along [110]. In contrast, electron transport is isotropic at ν=5/2 and 7/2 in the second Landau level. Finally, no

anisotropy is observed in the Hall resistance. These results are consistent with previous work [27-36].

In Figure 2, we show the tilted magnetic field dependence of R_{xx} and R_{yy} measured in the d=164nm sample in two configurations. In the first configuration, the in-plane magnetic field B_{ip} is parallel to [1-10] (or perpendicular to [110]). It can be seen in Figure 2(a) that R_{xx} and R_{yy} are almost the same in the regime of $4> \nu >2$ at zero tilt angle. With increasing tilt angle or B_{ip}, the R_{xx} minimum at $\nu=5/2$, measured along B_{ip}, increases and the QHE feature becomes weakened. By 75.9^{o}, a giant peak has developed at $\nu=5/2$ in R_{xx}. The R_{yy} at $\nu=5/2$, measured perpendicular to B_{ip}, remains a dip and displays a very weak B_{ip} dependence. In Figure 2(b), we show R_{xx} and R_{yy} at $\nu=5/2$ as a function of B_{ip}. Again, $R_{xx} \sim R_{yy}$ in the perpendicular B field (or $B_{ip}=0$). Under in-plane magnetic fields, R_{xx} and R_{yy} become anisotropic.

We then pulled out the sample and rotated it by 90^{o} and re-cooled it using the same cooling procedure. In this configuration [Figures 2(c) and 2(d)], the in-plane field is parallel to [110] (or perpendicular to [1-10]). Again, R_{xx} and R_{yy} are virtually the same at the zero tilt. Upon tilting, anisotropy in R_{xx} and R_{yy} develops with increasing tilt angle, the same as in the first configuration.

We summarize here that in the d=164 nm quantum well the 5/2 state becomes anisotropic in both configurations. And the hard axis is always parallel to B_{ip}, independent of

crystallographic directions. These results are consistent with those reported in Ref. [18,19].

We then examined two more samples of different d. In Figure 3, we show the results in the sample with the smallest d of 33 nm. When B_{ip} is parallel to [1-10] direction [Figures 3(a) and (b)], R_{xx} and R_{yy} display a similar in-plane field induced anisotropy as in Figures 2 (a) and (b). When B_{ip} is applied in [110] direction [Figures 3(c) and (d)], the 5/2 state is also destroyed. However, it remains isotropic even under high in-plane fields. Indeed, $R_{xx} \sim R_{yy}$ even when B_{ip} is larger than 8T. This is very different from that in Figures 2 (c) and (d).

To summarize the results in Figure 3, we observe that in the d=33nm sample the 5/2 FQHE state is destroyed by in–plane magnetic fields. It becomes anisotropic when B_{ip} is parallel to [1-10], but remains isotopic when B_{ip} is in [110] direction. This observation is consistent with the findings reported in Ref. [12].

In Figure 4, we plot the anisotropy factor (AF), defined as $AF = (R_{xx}-R_{yy})/(R_{xx}+R_{yy})$, as a function of decreasing d or increasing impact of modulation doping. The anisotropy develops in both in-plane field directions for d = 164 nm. As d is reduced to 52 nm, the anisotropy is fully developed (or $AF \approx 1$) when B_{ip} is in [1-10] direction. However, AF saturates to a value around 0.5 when B_{ip} // [110]. With d further reduced to 33 nm, AF is now almost zero for B_{ip} // [110] while close to 1 for B_{ip}//[1-10].

Our results in Figure 4 clearly demonstrate the distance between the modulation doping layers and quantum well is a determining factor in causing the anomalous B_{ip} induced anisotropy in high density samples. In the following we consider two previously proposed mechanisms [8, 37-39] that can explain this anomaly in the samples where the modulation doping layer effect is strong.

First, it was argued in Ref. [38] that the electric field between the 2DES and the modulation doping layers [37-39] could generate an anisotropic band mass, and this anisotropic mass can provide a symmetry breaking mechanism in magnetic field. As shown in Ref. [38], due to the "uniaxial stress" induced by this electric field, the GaAs bonds in [110] direction are stretched, while the bonds in [1-10] direction are shortened. As a consequence, the effective band mass is heavier in [1-10] direction and lighter in [110], which favors the stripes parallel to [110]. It can be expected that when d is large or n is low, the pinning force due to the band mass anisotropy is weaker than the de-pinning force induced by B_{ip}. Consequently, the stripes are locked perpendicularly to the direction of B_{ip}, as observed in the past. However, when d becomes smaller or n higher, the band mass anisotropy and, accordingly, the [110] pinning force increase. When B_{ip} is along [1-10], both B_{ip} and mass anisotropy help align the stripes perpendicular to B_{ip}. When B_{ip} is pointed to [110] direction, the re-orientation of stripes to [1-10] due to B_{ip} competes with the pinning to [110] due to the band mass anisotropy, which is now stronger due to higher n. As a result, it is possible that the stripes finally align themselves at an angle between [110] and [1-10] directions. This can give rise to an apparent isotropic electron transport.

For the second mechanism, we consider a possible quasiperiodic potential in the modulation doping layers by electron correlation [8]. Surface morphology studies [40-42] suggested that the periodic potential lines are in [1-10] direction. It is known that this periodic potential can cause an effect similar to an artificially modulated sample [8,40], and helps orientate the stripes perpendicular to the potential modulation [40,41,43,44]. When d is large, this periodic potential is weak and the reorientation of stripes in the presence of B_{ip} is dominant. As a consequence, the in-plane field induced stripes is determined by the direction of B_{ip}. When d is small, however, the periodic potential can provide a much stronger pinning force. With B_{ip} in [1-10] direction, or parallel to the potential modulation lines, pinning due to both B_{ip} and this periodic potential helps pin the stripes perpendicular to B_{ip}. When B_{ip} is perpendicular to the potential modulation or in [110] direction, the orientation of the 5/2 stripes is now determined by the competition of B_{ip} de-pinning and the quasiperiodic potential pinning. The outcome of this competition may again align the stripes along a direction between [110] and [1-10], giving rise to an isotropic electron transport.

In summary, we report results from a systematic tilted magnetic field study of the $\nu=5/2$ FQHE in a series of high quality GaAs quantum wells, in which the setback distance between the modulation doping layers and GaAs quantum well is varied from 33nm to 164nm. We have observed that in the sample of the shortest d electronic transport is anisotropic when B_{ip} is parallel to [1-10] crystallographic direction but remains more or less isotropic in the other direction of [110], consistent with previous work. In contrast, in the samples of larger d, electronic transport is anisotropic in both crystallographic

directions. Our results clearly show that the modulation doping layers do matter in the tilted magnetic field induced anisotropy in the 5/2 FQHE.

We thank Michael Manfra for helpful discussions. This work was supported by the Department of Energy, Office of Basic Energy Sciences, Division of Materials Sciences and Engineering. Sandia National Laboratories is a multi-program laboratory managed and operated by Sandia Corporation, a wholly owned subsidiary of Lockheed Martin Corporation, for the U.S. Department of Energy's National Nuclear Security Administration under contract DE-AC04-94AL85000. Sample growth at Princeton University was partially funded by the Gordon and Betty Moore Foundation, Keck foundation, as well as the National Science Foundation MRSEC Program through the Princeton Center for Complex Materials. A portion of the work was performed at the National High Magnetic Field Laboratory, which is supported by NSF Grant Nos. DMR-0084173 and ECS-0348289, the State of Florida, and DOE. We thank Tim Murphy, Ju-Hyun Park, and Glover Jones for experimental help.

References:

[1] H.L. Stormer, R. Dingle, A.C. Gossard, and W. Wiegmann, Conf. Ser. Inst. Phys. London **43**, 557 (1978).
[2] L.N. Pfeiffer and K.W. West, Physica E **20**, 57 (2003).
[3] D.C. Tsui, H.L. Stormer, and A.C. Gossard, Phys. Rev. Lett. **48**, 1559 (1982).
[4] R. B. Laughlin, Phys. Rev. Lett. **50**, 1395 (1983).
[5] F.□D.□M. Haldane, Phys. Rev. Lett. **51**, 605 (1995).
[6] B.□I. Halperin, Phys. Rev. Lett. **52**, 1583 (1984).
[7] J.□K. Jain, Phys. Rev. Lett. **63**, 199 (1989).
[8] Y.-W. Tan, H.L. Stormer, L.N. Pfeiffer, K.W. West, Phys. Rev. Lett. **98**, 036804 (2007).
[9] W. Pan, N. Masuhara, N. S. Sullivan, K. W. Baldwin, K.W. West, L. N. Pfeiffer, and D. C. Tsui, Phys. Rev. Lett. **106**, 206806 (2011).
[10] Gerardo Gamez and Koji Muraki, Phys. Rev. B **88**, 075308 (2013).
[11] N. Deng, G.□C. Gardner, S. Mondal, E. Kleinbaum, M.□J. Manfra, and G.□A. Csáthy,
Phys. Rev. Lett. **112**, 116804 (2014).
[12] Chi Zhang, T. Knuuttila, Yanhua Dai, R. R. Du, L. N. Pfeiffer, and K. W. West, Phys. Rev. Lett. **104**, 166801(2010).
[13] R. Willett, J. P. Eisenstein, H. L. Stormer, D. C. Tsui, A.C. Gossard, and J. H. English, Phys. Rev. Lett. **59**, 1776 (1987).
[14] W. Pan, J.-S. Xia, V. Shvarts, D. E. Adams, H. L. Stormer, D. C. Tsui, L. N. Pfeiffer, K. W. Baldwin, and K. W. West, Phys. Rev. Lett. **83**, 3530 (1999).
[15] G. Moore and N. Read, Nucl. Phys. B **360**, 362 (1991).
[16] C. Nayak, S.H. Simon, A. Stern, M. Freedman, and S. Das Sarma, Rev. Mod. Phys. **80**, 1083 (2008).
[17] J. P. Eisenstein, R. Willett, H. L. Stormer, D. C. Tsui, A. C. Gossard, and J. H. English, Phys. Rev. Lett. **61**, 997 (1988).
[18] W. Pan, R.R. Du, H.L. Stormer, D.C. Tsui, L.N. Pfeiffer, K.W. Baldwin, and K.W. West, Phys. Rev. Lett. **83**, 820 (1999).
[19] M.P. Lilly, K.B. Cooper, J.P. Eisenstein, L.N. Pfeiffer, and K.W. West, Phys. Rev. Lett. **83**, 824 (1999).
[20] C. R. Dean, B. A. Piot, P. Hayden, S. Das Sarma, G. Gervais, L. N. Pfeiffer, and K. W. West, Phys. Rev. Lett. **100**, 146803 (2008).
[21] J. Xia, V. Cvicek, J.P. Eisenstein, L.N. Pfeiffer, and K.W. West, Phys. Rev. Lett. **105**, 176807 (2010).
[22] G. Liu, C. Zhang, D. C. Tsui, I. Knez, A. Levine, R. R. Du, L. N. Pfeiffer, and K. W. West, Phys. Rev. Lett. **108**, 196805 (2012).
[23] E.H. Rezayi and F.D.M. Haldane, Phys. Rev. Lett. **84**, 4685 (2000).
[24] T. Jungwirth, A.H. MacDonald, L. Smrcka, and S.M. Girvin, Phys. Rev. B **60**, 15574 (1999).
[25] T.D. Stanescu, I. Martin, and P. Phillips, Phys. Rev. Lett. **84**, 1288 (2000).
[26] W. Pan, T. Jungwirth, H.L. Stormer, D.C. Tsui, A.H. MacDonald, S.M. Girvin, L. Smrcka, L.N. Pfeiffer, K.W. West, and K.W. Baldwin, Phys. Rev. Lett. **85**, 3257 (2000).
[27] M.M. Fogler, A.A. Koulakov, and B.I. Shklovskii, Phys. Rev. B **54**, 1853 (1996);

[28] R. Moessner and J. T. Chalker, Phys. Rev. B **54**, 5006 (1996).
[29] M. P. Lilly, K.B. Cooper, J.P. Eisenstein, L.N. Pfeiffer, and K.W. West, Phys. Rev. Lett. **82**, 394 (1999).
[30] R.R. Du, D.C. Tsui, H.L. Stormer, L.N. Pfeiffer, K.W. Baldwin, and K.W. West, Solid State Commun. **109**, 389 (1999).
[31] E. Fradkin and S.A. Kivelson, Phys. Rev. B **59**, 8065 (1999).
[32] H.A. Fertig, Phys. Rev. Lett. **82**, 3693 (1999).
[33] A.H. MacDonald and M.P.A. Fisher, Phys. Rev. B **61**, 5724 (2000).
[34] J. Zhu, W. Pan, H.L. Stormer, L.N. Pfeiffer, and K.W. West, Phys. Rev. Lett. **88**, 116803 (2002).
[35] H. Zhu, G. Sambandamurthy, L.W. Engel, D.C. Tsui, L.N. Pfeiffer, and K.W. West, Phys. Rev. Lett. **102**, 136804 (2009).
[36] I. V. Kukushkin, V. Umansky, K. von Klitzing, and J. H. Smet, Phys. Rev. Lett. **106**, 206804 (2011).
[37] H. Kroemer, arXiv:cond-mat/9901016
[38] B. Rosenow and S. Scheidl, Int. J. Mod. Phys. B **15**, 1905 (2001).
[39] S.P. Koduvayur, Y. Lyanda-Geller, S. Khlebnikov, G. Csathy, M.J. Manfra, L.N. Pfeiffer, K.W. West, and L.P. Rokhinson, Phys. Rev. Lett. **106**, 016804 (2011).
[40] R.L. Willett, J.W.P. Hsu, D. Natelson, K.W. West, and L.N. Pfeiffer, Phys. Rev. Lett. **87**, 126803 (2001).
[41] I.J. Maasilta, S. Chakraborty, I. Kuljanishvili, S.H. Tessmer, and M.R. Melloch, Phys. Rev. B **68**, 205328 (2003).
[42] K.B. Cooper, M.P. Lilly, J.P. Eisenstein, T. Jungwirth, L.N. Pfeiffer, K.W. West, Solid State Communications **119**, 89 (2001).
[43] Yoshioka, J. Phys. Soc. Jap. **70**, 2836 (2001).
[44] A. Endo and Y. Iye, Phys. Rev. B **66**, 075333 (2002).

Figure captions:

Figure 1: (a) shows the schematic of GaAs quantum well growth structure. The set-back distance (d) is defined between the edge of GaAs quantum well and the δ-doping layer. (b) shows the electron density (n) and mobility (μ) as a function of 1/d. We plot in (c) the R_{xx}, R_{yy}, and R_{xy} traces in the d=52 nm sample, where the electron mobility is the highest.

Figure 2: (a) shows R_{xx} and R_{yy} measured at various tilt angles in the d=164nm sample. The arrows mark the 5/2 and 7/2 states. The in-plane magnetic field (B_{ip}) direction is parallel to [1-10] direction. In Figure 2(b) we plot the R_{xx} and R_{yy} values at ν=5/2 as a function of B_{ip}. (c) is similar to (a), but for B_{ip} // [110]. (d) is similar to (b), for B_{ip}//[110].

Figure 3: (a) shows R_{xx} and R_{yy} measured at various tilt angles in the d=33nm sample. The arrows mark the 5/2 and 7/2 states. The in-plane magnetic field (B_{ip}) direction is parallel to [1-10] direction. In Figure 3(b) we plot the R_{xx} and R_{yy} values at ν=5/2 as a function of B_{ip}. (c) is similar to (a), but for B_{ip} // [110]. (d) is similar to (b), for B_{ip}//[110].

Figure 4: The anisotropy factor AF at ν=5/2, defined as $AF = (R_{xx}-R_{yy})/(R_{xx}+R_{yy})$, for three selected samples, where the impact of modulation doping layer increases with decreasing d.

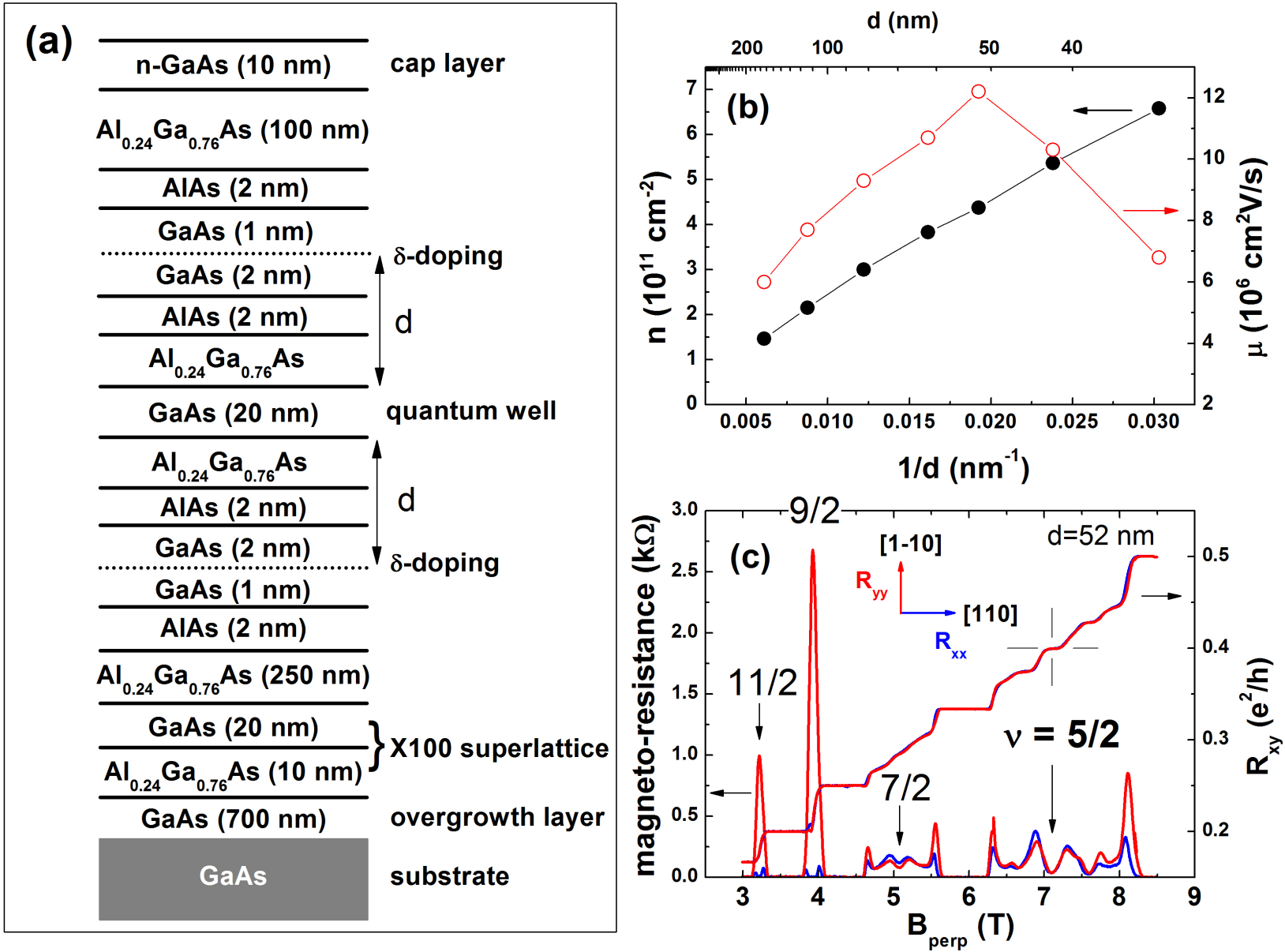
(a)
n-GaAs (10 nm)
cap layer
Al0.24Ga0.76As (100 nm)
AlAs (2 nm)
GaAs (1 nm)
δ-doping
GaAs (2 nm)
AlAs (2 nm)
Al0.24Ga0.76As
d
GaAs (20 nm)
quantum well
Al0.24Ga0.76As
AlAs (2 nm)
GaAs (2 nm)
d
δ-doping
GaAs (1 nm)
AlAs (2 nm)
Al0.24Ga0.76As (250 nm)
GaAs (20 nm)
Al0.24Ga0.76As (10 nm)
X100 superlattice
GaAs (700 nm)
overgrowth layer
GaAs
substrate
(b)
d (nm)
200
100
50
40
n (10^11 cm^-2)
μ (10^6 cm^2V/s)
1/d (nm^-1)
0.005
0.010
0.015
0.020
0.025
0.030
(c)
d=52 nm
9/2
11/2
7/2
ν = 5/2
[1-10]
[110]
Ryy
Rxx
magneto-resistance (kΩ)
Rxy (e^2/h)
Bperp (T)

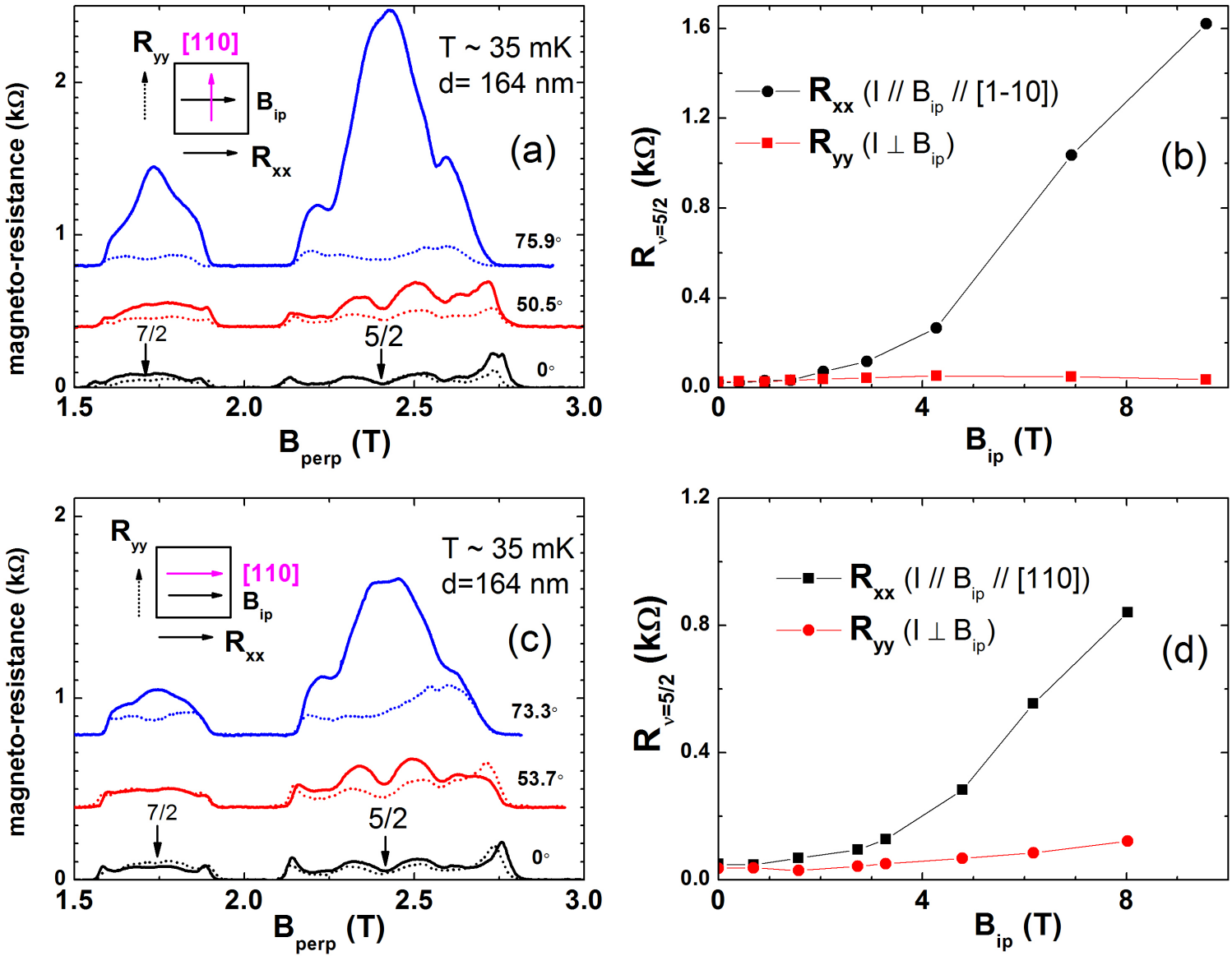
R_yy
[110]
B_ip
R_xx
T ~ 35 mK
d= 164 nm
(a)
75.9°
50.5°
0°
7/2
5/2
magneto-resistance (kΩ)
B_perp (T)
R_xx (I // B_ip // [1-10])
R_yy (I ⊥ B_ip)
(b)
R_ν=5/2 (kΩ)
B_ip (T)
R_yy
[110]
B_ip
R_xx
T ~ 35 mK
d=164 nm
(c)
73.3°
53.7°
0°
7/2
5/2
magneto-resistance (kΩ)
B_perp (T)
R_xx (I // B_ip // [110])
R_yy (I ⊥ B_ip)
(d)
R_ν=5/2 (kΩ)
B_ip (T)

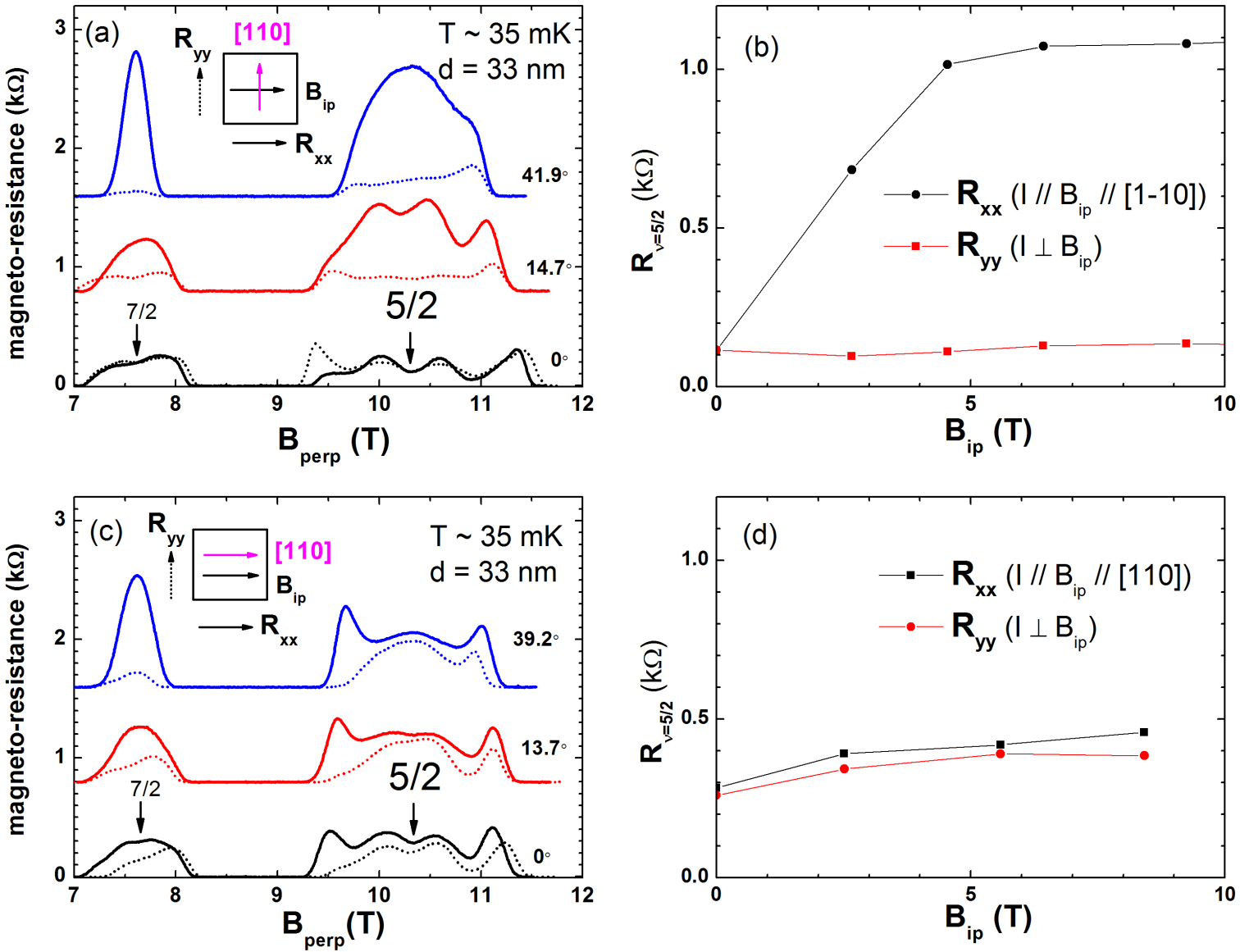
(a)
T ~ 35 mK
d = 33 nm
[110]
R_{yy}
B_{ip}
R_{xx}
41.9°
14.7°
0°
7/2
5/2
magneto-resistance (kΩ)
B_{perp} (T)
(b)
R_{xx} (I // B_{ip} // [1-10])
R_{yy} (I ⊥ B_{ip})
$R_{\nu=5/2}$ (kΩ)
B_{ip} (T)
(c)
T ~ 35 mK
d = 33 nm
[110]
R_{yy}
B_{ip}
R_{xx}
39.2°
13.7°
0°
7/2
5/2
magneto-resistance (kΩ)
B_{perp} (T)
(d)
R_{xx} (I // B_{ip} // [110])
R_{yy} (I ⊥ B_{ip})
$R_{\nu=5/2}$ (kΩ)
B_{ip} (T)

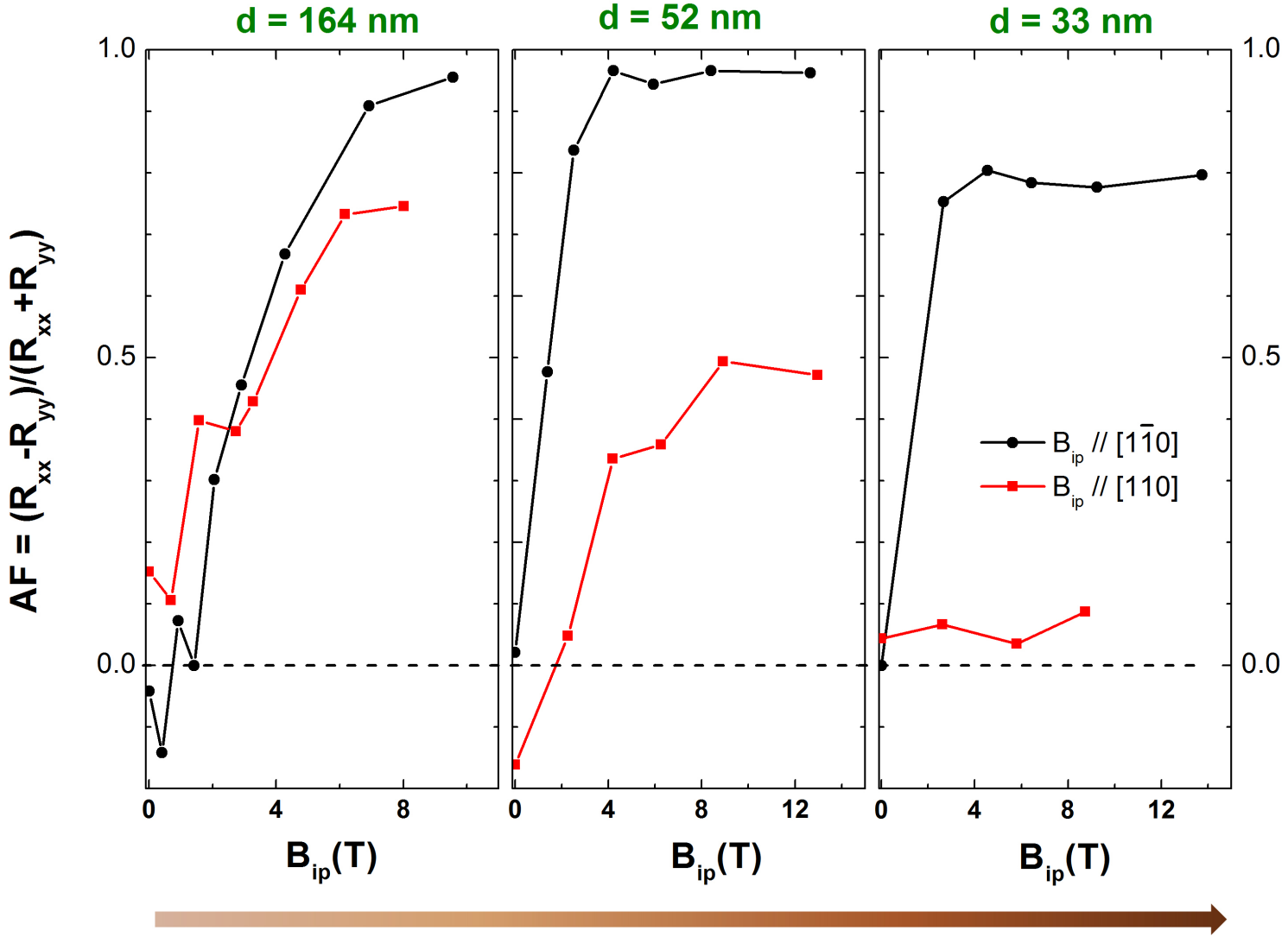
d = 164 nm
d = 52 nm
d = 33 nm
AF = (R_xx-R_yy)/(R_xx+R_yy)
1.0
0.5
0.0
0
4
8
12
B_ip(T)
B_ip // [1-10]
B_ip // [110]
decreasing d (increasing impact of modulation doping layer)